Identifcation of Pathways and Genes Associated With Meniscus Degeneration Using Bioinformatics Analyses

Hui Huang
Hainan General Hospital(Hainan Affiliated Hospital of Hainan Medical University)
Jiaxuan Zheng
Hainan General Hospital(Hainan Affiliated Hospital of Hainan Medical University)
Haiquan Tian
The Second People's Hospital of Changzhi
Yehan Fang
Hainan General Hospital(Hainan Affiliated Hospital of Hainan Medical University)
Wei Wang
Hainan General Hospital(Hainan Affiliated Hospital of Hainan Medical University)
Guangji Wang
Hainan General Hospital(Hainan Affiliated Hospital of Hainan Medical University)
Ming Deng
Renmin Hospital of Wuhan University
Jianping Lin (huangduosheng1958@163.com)
Hainan General Hospital(Hainan Affiliated Hospital of Hainan Medical University), Haikou 570311, Hainan Province, China

Research Article

Keywords: Meniscus, Degeneration, Differentially expressed genes, Bioinformatics analyses, Pathway

Posted Date: January 18th, 2021

DOI: https://doi.org/10.21203/rs.3.rs-145945/v1

Abstract

There are few studies on the genetic changes of meniscus degeneration. We used anterior cruciate ligament resection of Wuzhishan pig to prepare a meniscus degeneration model, and applied gene chip technology to detect differentially expressed genes in degenerative meniscus tissue. Then we applied GO analysis, Pathway analysis, Core gene network analysis and Relevant miRNAs analysis to discover relevant regulatory networks of meniscus degeneration. As a result, we detected 893 differentially expressed genes, mainly involving hormone, apoptosis, inflammation and other mechanisms, and obtained MUC13, Inflammatory mediator regulation of TRP channels, MDFI, mir-335-5p and so on that may play a key role. In summary, we have established a reliable animal model of meniscus degeneration and found that meniscus degeneration involves several possible molecular mechanisms, which will provide molecular targets for further research of the disease in the future.

Introduction

The meniscus has the functions of buffering load, absorbing impact, decompressing and improving joint stability. And the blood circulation of the meniscus is poor, the healing ability is limited, and it is easy to degenerate. The degenerative meniscus not only cannot fully protect the knee joint, but also tends to tear itself, leading to knee cartilage damage, pain, and restricted knee movement[1,2]. In addition, Meniscus degeneration can lead to osteoarthritis[3]. Therefore, how to protect the meniscus and delay the degeneration of the meniscus has important scientific significance for preventing meniscus injury in young and middle-aged patients and alleviating the symptoms of elderly patients with knee arthritis.

Meniscus and articular cartilage are very similar in tissue composition, many researchers speculate that meniscus degeneration may be similar to cartilage degeneration, and the imbalance between anabolism and catabolism leads to degeneration[4,5]. But the specific mechanism is not clear. Trauma, chronic inflammation, apoptosis and so on may be involved unilaterally or in multiple ways, and there are countless kinds of genes that may play a role, which brings great trouble to the research of meniscus degeneration mechanism[6,7]. With the advantages of large amount of information, reliable operation and repeatability, gene chip technology has been successfully used in gene expression detection, DNA sequencing, search for new genes, diagnosis of diseases and other research fields[8]. This study used gene chip technology to screen differentially expressed genes (DEGs) between normal meniscus and degenerated meniscus, and tried to analyze the mechanism of meniscal degeneration to provide theoretical basis for the diagnosis, prevention and treatment of meniscal degeneration.

Results

Gross morphological observation

In the normal meniscus group, the meniscus was smooth and complete, with a white and shiny surface, without any signs of degeneration. In the degenerative meniscus group, the surface of meniscus was rough, the color was dim, the elasticity was poor, and there were some small defects and erosion (Fig. 1).

Figure 1. (a) In the normal meniscus group, the meniscus was crescent shaped, with complete and smooth surface, no tear, white color and good elasticity. And the medial part of the meniscus was thin and the lateral part was thick. (b) In the degenerative meniscus group, the color of the meniscus was light yellow, the elasticity was worse than that of the normal meniscus, the surrounding synovial membrane was congested and edema, the inner part was thinner with uneven wear, and the free edge was incomplete and cracked.

Histological examination

In the normal meniscus group, HE staining of the meniscus showed normal meniscus tissue. In the degenerative meniscus group, HE staining of the meniscus showed disorder, uneven staining and sparse arrangement of collagen fibers, disorder, reduction and swelling of chondrocytes, reduction or disappearance of cartilage lacunae, increased local fibers and hyaline changes, which were consistent with meniscal degeneration (Fig. 2).

Figure 2. (a-b) The HE staining of normal meniscus tissue. The chondrocyte nucleus was large and round, the cell distribution was regular, the collagen fibers were abundant, and the fiber bundles were thick and neat. (c-f) The HE staining of degenerative meniscus. The arrangement of collagen fibers was disordered, the staining was uneven, and the arrangement was sparse; the chondrocytes were arranged disorderly and reduced, and the visible cells were swollen, the cartilage lacuna was reduced or disappeared, and the local area was fibrotic and hyalinized. a: x40, b: x100, c: x40, d: x100, e: x200, f: x400.

Quality control

For RNA quantification and quality assurance performed by NanoDrop ND-1000, the ratio of A260/A280 for all samples was close to 2.0, and the ratio of O.D. A260/A230 was greater than 1.8. The result of Agilent 2100 Bioanalyzer showed that all RINs ≥ 6.3, indicating that the integrity of total RNA was good and there was no obvious degradation, so follow-up experiments could be carried out (Table 1).

Table 1. RNA quality control result

Sample ID	OD260/280 Ratio	OD260/230 Ratio	Conc. (ng/μl)	RIN	Pass or Fail
NM1	2.00	1.90	319.41	6.9	Pass
NM2	1.88	1.96	195.83	6.5	Pass
NM3	2.00	1.99	314.36	6.5	Pass
NM4	2.02	1.91	299.40	6.4	Pass
NM5	2.01	1.97	335.84	6.3	Pass
NM6	1.94	1.85	164.94	7.2	Pass
NM7	2.00	1.94	316.15	6.3	Pass
DM1	1.97	1.92	358.41	7.3	Pass
DM2	2.02	1.97	721.61	7.5	Pass
DM3	2.03	1.90	400.45	6.3	Pass
DM4	1.83	1.96	112.25	7.2	Pass
DM5	1.98	1.89	267.03	6.5	Pass
DM6	1.86	1.90	251.31	6.4	Pass
DM7	2.01	2.07	345.64	6.7	Pass

NM: normal meniscus; DM: degenerative meniscus

DEGs

There were 893 DEGs in the two groups, including 537 up-regulated genes and 356 down-regulated genes. The result was showed in the volcano plot and the dendrogram(Fig. 3). The top 10 most significant genes were cyp2c33, gcnt7, ncdn, exd3, MUC13, ppp1r3d, nphp3, upb1, CD81 and prph (Table 2).

Figure 3. (a) The volcano plot. Red and green represent DEGs; the downregulated DEGs are green, and the upregulated DEGs are red. (b) The dendrogram. The ordinate represents the grouping information of the sample. Red indicates high relative expression and green indicates low relative expression. NM: normal meniscus; DM: degenerative meniscus.

Table 2. The top 10 most significant genes.

ProbeName	P-value	FDR	Fold Change	Regulation	GeneSymbol	Rank
A_72_P526917	1.2593E-07	0.000537464	2.0593695	up	CYP2C33	1
A_72_P362758	1.38326E-07	0.000537464	3.2506906	up	GCNT7	2
A_72_P050406	6.10533E-07	0.001031403	2.5418055	up	NCDN	3
A_72_P258107	8.6355E-07	0.001198329	2.5599119	up	EXD3	4
A_72_P165116	9.46523E-07	0.001225904	2.046065	up	MUC13	5
A_72_P442485	1.08108E-06	0.001272895	2.2891991	up	PPP1R3D	6
A_72_P222892	1.13988E-06	0.001302652	2.0178437	up	NPHP3	7
A_72_P234107	1.23101E-06	0.001328635	2.5152315	up	UPB1	8
A_72_P496803	1.4119E-06	0.001443671	3.0181273	up	CD81	9
A_72_P352838	1.81842E-06	0.001613149	2.4487246	up	PRPH	10

GO analysis

A total of 55 biological processes enriched by the DEGs were obtained. The top 10 biological processes were cell response to hormone stimulus, response to hormone, sex determination, muscle fiber development, mehcheme morphogenesis, cell response to endogenous stimulus, C21 steroid hormone metallic process, neuropeptide signaling pathway, negative regulation, respectively of reactive oxygen species metallic process and regulation of nitric oxide biosynthetic process (Table 3).

Table 3. The enriched GO terms for the DEGs.

Term	Count	P-value	Regulation	Rank
cellular response to hormone stimulus	7	0.000311929	Up	1
response to hormone	7	0.001152029	Up	2
sex determination	2	0.001281445	Down	3
muscle fiber development	2	0.002753211	Down	4
mesenchyme morphogenesis	2	0.002753211	Down	5
cellular response to endogenous stimulus	8	0.003566943	Up	6
C21-steroid hormone metabolic process	2	0.003588081	Up	7
neuropeptide signaling pathway	3	0.003940886	Up	8
negative regulation of reactive oxygen species metabolic process	2	0.004359628	Up	9
regulation of nitric oxide biosynthetic process	2	0.007086781	Up	10
response to endogenous stimulus	8	0.007145167	Up	11
negative regulation of reproductive process	2	0.008950734	Down	12
nitric oxide biosynthetic process	2	0.009235862	Up	13
nitric oxide metabolic process	2	0.009235862	Up	14
reactive nitrogen species metabolic process	2	0.009235862	Up	15
gland development	4	0.010284414	Up	16
hormone metabolic process	3	0.011308564	Up	17
male gonad development	2	0.011498663	Down	18
development of primary male sexual characteristics	2	0.011498663	Down	19
regulation of reactive oxygen species biosynthetic process	2	0.011638114	Up	20
body fluid secretion	2	0.012931151	Up	21
striated muscle cell development	2	0.013594657	Down	22
hormone biosynthetic process	2	0.015695135	Up	23
male sex differentiation	2	0.016626965	Down	24
muscle cell development	2	0.016626965	Down	25
reproductive structure development	3	0.017568602	Down	26
reproductive system development	3	0.017988302	Down	27
cellular hormone metabolic process	2	0.018688631	Up	28
regulation of hormone levels	3	0.018844593	Down	29
reactive oxygen species biosynthetic process	2	0.020268615	Up	30
epithelial cell differentiation	3	0.020624915	Down	31
neurotransmitter biosynthetic process	2	0.021902613	Up	32
feeding behavior	2	0.023589533	Up	33

response to chemical	14	0.023617031	Up	34
cellular response to chemical stimulus	11	0.023892904	Up	35
hormone metabolic process	2	0.026281932	Down	36
bone remodeling	2	0.027117856	Up	37
striated muscle cell differentiation	2	0.033355701	Down	38
tissue development	5	0.035003106	Down	39
gonad development	2	0.035500212	Down	40
development of primary sexual characteristics	2	0.035500212	Down	41
mammary gland development	2	0.036791312	Up	42
mesenchyme development	2	0.038815337	Down	43
regulation of reproductive process	2	0.038815337	Down	44
muscle organ development	2	0.041089286	Down	45
response to oxygen-containing compound	6	0.041364725	Up	46
hormone-mediated signaling pathway	2	0.043140041	Up	47
neurotransmitter metabolic process	2	0.043140041	Up	48
regulation of reactive oxygen species metabolic process	2	0.043140041	Up	49
response to peptide	3	0.048362819	Up	50
body morphogenesis	1	0.048805944	Down	51
forebrain neuron differentiation	1	0.048805944	Down	52
regulation of interleukin-4 production	1	0.048805944	Down	53
positive regulation of mitotic nuclear division	1	0.048805944	Down	54
labyrinthine layer morphogenesis	1	0.048805944	Down	55

Pathway analysis

A total of 36 pathways were affected by the alteration of the gene expression. The top 10 pathways are Type II diabetes mellitus, Thyroid hormone synthesis, Taste transduction, Prolactin signaling pathway, Longevity regulating pathway, Ovarian steroidogenesis, Neuroactive ligand-receptor interaction, Inflammatory mediator regulation of TRP channels, Pantothenate and CoA biosynthesis and Cocaine addiction (Table 4).

Table 4. The enriched pathways for the DEGs.

Definition	Fisher P-value	regulation	Rank
Type II diabetes mellitus	0.000759595	Up	1
Thyroid hormone synthesis	0.002669959	Down	2
Taste transduction	0.002858715	Up	3
Prolactin signaling pathway	0.003352503	Up	4
Longevity regulating pathway	0.007875137	Up	5
Ovarian steroidogenesis	0.009215694	Up	6
Neuroactive ligand-receptor interaction	0.01021098	Up	7
Inflammatory mediator regulation of TRP channels	0.01098087	Up	8
Pantothenate and CoA biosynthesis	0.01205545	Up	9
Cocaine addiction	0.01468413	Down	10
Metabolism of xenobiotics by cytochrome P450	0.01528523	Down	11
Legionellosis	0.01844662	Down	12
AMPK signaling pathway	0.02220957	Up	13
Bile secretion	0.02225764	Up	14
Glycerolipid metabolism	0.02257206	Down	15
Chemical carcinogenesis	0.02329364	Down	16
Adipocytokine signaling pathway	0.0249136	Up	17
Amphetamine addiction	0.02627419	Down	18
Acute myeloid leukemia	0.02627419	Down	19
Adherens junction	0.03020581	Down	20
Drug metabolism - other enzymes	0.03062382	Up	21
Insulin signaling pathway	0.0323184	Up	22
African trypanosomiasis	0.03438215	Up	23
Dilated cardiomyopathy (DCM)	0.0360517	Up	24
Primary immunodeficiency	0.03632543	Up	25
Insulin secretion	0.03717241	Up	26
GABAergic synapse	0.03831094	Up	27
Phospholipase D signaling pathway	0.0386556	Up	28
Salmonella infection	0.03961531	Down	29
Protein digestion and absorption	0.04064128	Up	30
GnRH signaling pathway	0.04304219	Up	31
Progesterone-mediated oocyte maturation	0.04304219	Up	32
Protein digestion and absorption	0.04516019	Down	33

Morphine addiction	0.04551314	Up	34
Endocrine resistance	0.0467747	Up	35
Hematopoietic cell lineage	0.04706952	Down	36

Core gene network and Relevant miRNA analysis

Core network analysis yielded 40 core genes, of which the gene MDFI had the largest number of connections, indicating that it was in the most central position (Fig. 4, Table 5). Relevant miRNA analysis yielded 101 related miRNAs, among which miR-335-5p was the most connected related miRNA (Fig. 5, Table 6).

Table 5. The Correspondence and data source of the Core genes.

Gene 1	Protein 1	Gene 2	Protein 2	Relationship	Experiment	Source
MDFI	Q99750	GREM1	O60565	protein interaction	two hybrid array	PMID:unassigned1304
MDFI	Q99750	ZNF408	Q9H9D4	protein interaction	two hybrid array	PMID:19060904
MDFI	Q99750	ZNF408	Q9H9D4	protein interaction	two hybrid array	PMID:unassigned1304
MDFI	Q99750	ZNF408	Q9H9D4	protein interaction	two hybrid pooling approach	PMID:16189514
MDFI	Q99750	RIPPLY1	Q0D2K3	protein interaction	two hybrid array	PMID:unassigned1304
MDFI	Q99750	ADRA2C	P18825	protein interaction	two hybrid array	PMID:unassigned1304
SSX2IP	Q9Y2D8	ZNF408	Q9H9D4	protein interaction	two hybrid array	PMID:unassigned1304
IL2RG		PRL		activation		pathway_id:hsa04630
PRL		IL2RG		activation		pathway_id:hsa04630
LEF1		CTNND2		inhibition		pathway_id:hsa04310
CTNND2		LEF1		inhibition		pathway_id:hsa04310
CTNND2	Q9UQB3	TTR	P02766	protein interaction	two hybrid	PMID:21900206
ZNF408	Q9H9D4	MDFI	Q99750	protein interaction	two hybrid array	PMID:19060904
ZNF408	Q9H9D4	MDFI	Q99750	protein interaction	two hybrid array	PMID:unassigned1304
ZNF408	Q9H9D4	MDFI	Q99750	protein interaction	two hybrid pooling approach	PMID:16189514
ZNF408	Q9H9D4	SSX2IP	Q9Y2D8	protein interaction	two hybrid array	PMID:unassigned1304
RIPPLY1	Q0D2K3	MDFI	Q99750	protein interaction	two hybrid array	PMID:unassigned1304
ADRA2C	P18825	MDFI	Q99750	protein interaction	two hybrid array	PMID:unassigned1304
PDYN		ATF4		activation expression		pathway_id:hsa05030
PDYN		ATF4		activation expression		pathway_id:hsa05031
RAB33A	Q14088	RTN4	Q9NQC3	protein interaction	two hybrid pooling approach	PMID:16189514
RTN4	Q9NQC3	RAB33A	Q14088	protein interaction	two hybrid pooling approach	PMID:16189514
CFAP58	Q5T655	RIPPLY1	Q0D2K3	protein interaction	two hybrid array	PMID:unassigned1304

RSPH14	Q9UHP6	TRIM69	Q86WT6	protein interaction	two hybrid array	PMID:unassigned1304
TRIM69	Q86WT6	RSPH14	Q9UHP6	protein interaction	two hybrid array	PMID:unassigned1304
HTR2C	P28335	RTN4	Q9NQC3	protein interaction	ubiquitin reconstruction	PMID:28298427
SLC2A4		ADIPOQ		indirect relationship		pathway_id:hsa04930
TG		ATF4		activation expression		pathway_id:hsa04918
ADIPOQ	Q15848	FASN	P49327	protein interaction	two hybrid array	PMID:unassigned1304
AFDN		SSX2IP		binding/protein interaction		pathway_id:hsa04520
SSX2IP		AFDN		binding/protein interaction		pathway_id:hsa04520
SSX2IP	Q9Y2D8	ZNF408	Q9H9D4	protein interaction	two hybrid array	PMID:unassigned1304
ARID2	Q68CP9	CD14	P08571	protein interaction	anti tag coimmunoprecipitation	PMID:26496610
CD14	P08571	ARID2	Q68CP9	protein interaction	anti tag coimmunoprecipitation	PMID:26496610
CD14	P08571	CD81	P60033	protein interaction	fluorescent resonance energy transfer	PMID:11745332
ATF4	P18848	CEP83	Q9Y592	protein interaction	two hybrid array	PMID:unassigned1304
ATF4	P18848	TTR	P02766	protein interaction	two hybrid pooling approach	PMID:16189514
TTR	P02766	ATF4	P18848	protein interaction	two hybrid pooling approach	PMID:16189514
CEP83	Q9Y592	ATF4	P18848	protein interaction	two hybrid array	PMID:unassigned1304
ATXN2	Q99700	PABPC1	P11940	direct interaction	x-ray crystallography	PMID:20181956
ATXN2	Q99700	PABPC1	P11940	protein interaction	surface plasmon resonance	PMID:20181956
PABPC1	P11940	ATXN2	Q99700	direct interaction	x-ray crystallography	PMID:20181956
PABPC1	P11940	ATXN2	Q99700	protein interaction	surface plasmon resonance	PMID:20181956
CCR10	P46092	S100A10	P60903	protein interaction	pull down	PMID:26941067
S100A10	P60903	CCR10	P46092	protein interaction	proximity ligation assay	PMID:26941067
CD81	P60033	CD14	P08571	protein interaction	fluorescent resonance energy transfer	PMID:11745332

COBLL1	Q53SF7	DLG3	Q92796	protein interaction	anti tag coimmunoprecipitation	PMID:26496610
DLG3	Q92796	COBLL1	Q53SF7	protein interaction	anti tag coimmunoprecipitation	PMID:26496610
CYP17A1		ATF4		activation expression		pathway_id:hsa04927
CYP17A1		ATF4		activation expression		pathway_id:hsa04934
CYP17A1		CYP2E1		compound		pathway_id:hsa00140
CYP17A1		NR5A1		activation expression		pathway_id:hsa04927
CYP17A1		NR5A1		activation expression		pathway_id:hsa04934
CYP2E1		CYP17A1		compound		pathway_id:hsa00140
CYP2E1		EPHX1		compound		pathway_id:hsa00980
NR5A1		CYP17A1		Activation expression		pathway_id:hsa04927
NR5A1		CYP17A1		activation expression		pathway_id:hsa04934
CES1		CYP2E1		compound		pathway_id:hsa00983
EPHX1		CYP2E1		compound		pathway_id:hsa00980
GREM1	O60565	MDFI	Q99750	protein interaction	two hybrid array	PMID:unassigned1304

Table 6. The Correspondence and data source of miR-335-5p

MiRNA name	Target gene name	Experimental verification method	PMID
miR-335-5p	ABCC8	Microarray	18185580
miR-335-5p	ACE	Microarray	18185580
miR-335-5p	ADCY6	Microarray	18185580
miR-335-5p	ADGRE3	Microarray	18185580
miR-335-5p	AFDN	Microarray	18185580
miR-335-5p	CD14	Microarray	18185580
miR-335-5p	CFAP58	Microarray	18185580
miR-335-5p	CPEB4	Microarray	18185580
miR-335-5p	CYP2E1	Microarray	18185580
miR-335-5p	DLG3	Microarray	18185580
miR-335-5p	ESRP1	Microarray	18185580
miR-335-5p	EXD3	Microarray	18185580
miR-335-5p	GABBR1	Microarray	18185580
miR-335-5p	MACF1	Microarray	18185580
miR-335-5p	MDFI	Microarray	18185580
miR-335-5p	MLN	Microarray	18185580
miR-335-5p	MYOD1	Microarray	18185580
miR-335-5p	MYOT	Microarray	18185580
miR-335-5p	NCDN	HITS-CLIP	27418678
miR-335-5p	PNLIP	Microarray	18185580
miR-335-5p	PPP1R3D	Microarray	18185580
miR-335-5p	PTK2B	Microarray	18185580
miR-335-5p	SLC2A4	Microarray	18185580
miR-335-5p	SLC35A5	HITS-CLIP	23313552
miR-335-5p	SLC7A9	Microarray	18185580
miR-335-5p	SPTB	Microarray	18185580
miR-335-5p	TRIM40	Microarray	18185580
miR-335-5p	TRIM69	Microarray	18185580
miR-335-5p	TSPAN15	Microarray	18185580
miR-335-5p	ZNF609	Microarray	18185580

Real-time RT-PCR

In order to verify the reliability of the microarray results, the expression levels of the seven mRNAs (GCNT7, NCDN, EXD3, MUC13, PPP1R3D, NPHP3 and CD81) detected by RT-PCR were equivalent to the microarray data. And the difference of mRNA expression between the degenerative meniscus group and the normal meniscus group was statistically significant ($P < 0.05$) (Table 7).

Table 7. Primer and differential expression of mRNA

Gene	Primer(5' - 3')	Sham (x±s,n=7)	OA (x±s,n=7)	P-value
GAPDH	F:5′ TCTCTGCTCCTCCCCGTT 3′ R:5′ CGGCCAAATCCGTTCACT 3′			
GCNT7	F:5' GGCTTACACTGGCTTTAGGAG 3'	2.41±0.80	5.92±1.44	0.000
	R:5' AGTTTGGCTTGTCTTGGATTTA 3'			
NCDN	F:5' AGACCTGCTGTCACATCTTCCTC 3'	0.47±0.33	3.41±1.44	0.000
	R:5' AGCGACGCCATCAGAGTGTT 3'			
EXD3	F:5' GCATTTCAACGTGCGTGTCA 3'	0.26±0.17	1.33±0.41	0.000
	R:5' CGAGCTGCTTCATCATGTCCTT 3'			
MUC13	F:5' ATCTGCCAAGCGTGTCCATT 3'	0.02±0.02	0.14±0.11	0.014
	R:5' TGCAATCACCAGGCTGAGAA 3'			
PPP1R3D	F:5' GTCAAGGTGTTCAACGCGGG 3'	3.33±2.39	14.75±3.87	0.000
	R:5' GCCAGTCCGAGAAGGTGTAG 3'			
NPHP3	F:5' TGAACTGGGCGTGCTCTACTA 3'	1.97±0.94	5.04±1.72	0.001
	R:5' TGCTCGTCTCCGAATGTCTAA 3'			
CD81	F:5' ACTACCAGCCTCCTCTACCTG 3'	47.33±53.47	225.55±99.88	0.001
	R:5' ACAGGCAAAGAGGATCACGA 3'			

F: forword primer; R: reverse primer

Discussion

In this study, an Agilent-026440 Sus scrofa (Pig) Oligo Microarray v2 (Probe Name version) chip was used to detect the DEG of degenerative meniscus tissue. The results showed that there were 893 DEGs between the meniscus degeneration group and the normal group, of which 537 genes were up-regulated, 356 genes were down-regulated. We found 10 genes with the most significant expression. They are CYP2C33, GCNT7, NCDN, EXD3, MUC13, PPP1R3D, NPHP3, UPB1, CD81 and PRPH. Among them, we are interested in MUC13. The transmembrane mucin encoded by MUC13 has a variety of physiological functions, mainly to lubricate and protect the mucosal epithelium. Under pathological conditions, MUC13 expression is abnormal and participates in the occurrence and development of inflammation and tumors[9,10]. Our study found that MUC13 is highly expressed in degenerative meniscus tissues, suggesting that MUC13 may play an important role in it, presumably through the anti-inflammatory effect of MUC13. IL-8 is an important inflammatory factor. MUC13

promotes NF-κB activity through NF-κB-dependent pathways and increases IL-8 production. OA synovial fluid contains high levels of IL-6 and IL-8. The increased expression of IL-8 has a chemotactic effect on inflammatory cells and stimulates the secretion of IL-6, thereby promoting joint inflammation[11]. Therefore, MUC13 may play a role in degenerative meniscus tissue through the anti-inflammatory effect of MUC13.

According to the GO analysis results, 55 BPs were significantly expressed. After comprehensive analysis, DEGs participated in cellular response to hormone stimulus, response to hormone, sex determination, cellular response to endogenous stimulus, C21-steroid hormone metabolic process, neuropeptide signaling pathway, negative regulation of reactive oxygen species metabolic process, regulation of nitric oxide biosynthetic process, response to endogenous stimulus, negative regulation of reproductive process, nitric oxide biosynthetic process, nitric oxide metabolic process, reactive nitrogen species metabolic process, regulation of hormone levels, regulation of reactive oxygen species metabolic process, and regulation of interleukin-4 production. It is suggested that hormones, apoptosis, oxidation and other mechanisms are involved in the meniscus degeneration process. Studies[12-14] have reported that the inhibitory effect of sex hormones seems to be related to cystic degeneration of meniscus tissue, and growth hormone and parathyroid hormone have effects on meniscus and chondrocytes.

NO is the main cause of human articular chondrocyte apoptosis[15-18]. These studies are consistent with our finding. The regulatory biosynthesis process of nitric oxide is one of the most enriched biological processes in GO analysis. Studies have shown that NO induces chondrocyte apoptosis, and NO is the main cause of human articular chondrocyte apoptosis[15,19-23]. Our study shows that the biological process involved in meniscus degeneration involves NO, suggesting that NO-induced apoptosis also occurs in meniscus cells, which could eventually lead to the degeneration of meniscus tissue. The consistency between our finding and previous findings provides strong support for our hypothesis that degenerate meniscus cells are different from normal meniscus cells and may play an active role in the development of OA, in order to verify this finding , further research is still needed.

Inflammatory mediator regulation of TRP channels is one of the 10 lowest p-values in Pathway analysis. As a variety of cellular signal receptors, it plays a very important role in the inflammatory response[24,25]. This study found that inflammatory mediator regulation of TRP channels were upregulated in the meniscus of swine OA, suggesting that degeneration of the meniscus involves TRP channels and is associated with inflammatory responses.

Our research found MDFI and miR-335-5p, both of which regulate the WNT signaling pathway[26,27], which is the core signal pathway of OA synovitis[28-30]. This shows that synovitis and meniscal degeneration may have similar mechanisms of action. Synovial and meniscal tissues are also involved in the pathogenesis of OA. Pilar Tornero-Esteban's[31] study shows correlation between miR-335-5p expression and OA. Our study found a strong correlation between miR-335-5p and meniscus degeneration. MiR-335-5p could play an important role in meniscus degeneration, indicating that miR-335-5p may become a new target for clinical prevention and treatment of meniscus degeneration. The specific mechanism and how to mediate meniscus degeneration are the next research the key of.

This study has shortcomings. The experimental study uses a Wuzhishan pig meniscus degeneration model. The knee joint is different from humans in biomechanics, so the animal model research cannot be completely equivalent to the study of meniscus degeneration's patients. In addition, this model is more similar to traumatic meniscus degeneration, such as human meniscus and cruciate ligament injury, rather than primary meniscus degeneration. However, compared with many shortcomings such as the ethical issues involved in the study of human specimens, the lack of sample size, the obvious heterogeneity of specimens, and the difficulty of obtaining specimens in special parts, this animal model is an ideal research tool.

In summary, it is necessary to better understand the pathogenesis of meniscus degeneration, identify potential drug targets, and regulate gene expression of meniscus degeneration. This study is the first time that the whole gene spectrum

analysis of the meniscus tissue has been performed in the Wuzhishan pig animal. Our findings expand current understanding of the genetic mechanisms of meniscus degeneration. Therefore, these data provide a basis for future studies on the function of a large number of newly discovered genetic materials in the pathogenesis of meniscal degeneration and the suitability of the target as a drug target for meniscal degeneration.

Materials And Methods

Animals

A total of 14 healthy adult male Hainan Wuzhishan pigs (Institute of Animal Husbandry and Veterinary Medicine, Hainan Academy of Agricultural Sciences, China) were randomly divided into normal meniscus group and meniscus degeneration group. Anterior cruciate ligament resection was done in the meniscus degeneration group, and only the skin was cut in the normal meniscus group. The weight of each pig was 15-18kg, the age was 6-7 months, and normal illumination and diet and non-single cage feeding were given. The breeding environment temperature was 20-28 degrees centigrade. All pigs were sacrificed 24 weeks after the operation. All operations were performed under pentobarbital sodium anesthesia. The ethics committee had approved the experiment (Ethics Committee of Hainan Provincial People's Hospital of China, Ethical approval No: Med-Eth-Re [2018] 01). All methods were performed in accordance with the relevant guidelines and regulations of the ethics committee.

Gross morphological observation and HE staining

The medial meniscus was taken out and the smoothness, gloss and color of the surface to be observed. After a little cleaning, it was fixed with 10% formalin. After 72 hours, it was decalcified, dehydrated, and embedded in paraffin, and then sectioned. After HE staining, the morphological and structural changes of the tissue were observed under a microscope.

RNA extraction

According to the manufacturer's requirements, TRIzol RNA isolation reagent (Invitrogen, Carlsbad, CA, USA) was used to isolate total RNA from meniscal tissue. Quality control was performed by NanoDropND-1000 and Agilent 2100 Bioanalyzer.

Microarray

The Pig Gene Expression 4x44K Microarray V2 (Agilent Technologies, Santa Clara, CA, USA) were used to compare mRNA expression profiles, respectively, in normal and degenerative meniscus tissue. Microarray analysis was performed by GCBI analysis platform (Shanghai, China, https://www.gcbi.com.cn). The data have been deposited in the NCBI Gene Expression Omnibus and are accessible through GEO Series accession number GSE156132.

Strategy

The flow chart of the analysis was shown in the Fig. 6. First, the differentially expressed gene analysis used the two samples Welch's t-test (unequal variances) to identify significantly different mRNAs which were screened by $p < 0.05$, fold change > 1.5 and FDR < 0.05 and sorted by p value. Second, the gene ontology system is used to classify these differentially expressed genes according to their biological functions. Similarly, pathway analysis was used to identify affected KEGG pathways. Third, differential expression genes were further analyzed by core gene network analysis and related miRNAs analysis. The core gene network analysis displays the interaction relationship between the input genes, making it easier to understand the core genes of the input genes. The core network is based on the relationship between genes and genes that have database basis and literature basis in Pubmed, Mesh, KEGG and other databases. Related miRNAs analysis show at least two miRNAs that interact with the input gene. Related miRNAs are based on the

relationship between genes and miRNAs that are documented in Pubmed, miRBase and other databases, so as to construct a network of related miRNAs. All of the data mentioned above were analyzed by GCBI analysis platform.

Real-time RT-PCR

Changes in the expression of selected genes (GCNT7, NCDN, EXD3, MUC13, PPP1R3D, NPHP3 and CD81) were confirmed by RT-PCR. The 7 genes were chosen because they had the lowest p-value. TRIZOL reagent (Invitrogen, Carlsbad, CA, USA) was used to extract total RNA from meniscus tissue, and then 500ng RNA was taken to synthesize cDNA. PCR was performed on a ViiA 7 Real-time PCR System (Applied Biosystems, Foster City, CA, USA) using a 2X PCR master mix (Arraystar, Rockvile,MD, USA). The primers were chemically synthesized by Kangcheng, Shanghai, China and are listed in Table 7. GAPDH was used as internal controls to determine the relative expression of target mRNA. All reactions were repeated three times.

Statistical Analysis

The data of PT-PCR was analyzed using SPSS 19.0 software, and the counting data were expressed as ($x \pm s$). One-way ANOVA was used for comparison between two groups, and $P < 0.05$ indicated statistical difference.

Declarations

Acknowledgements: The authors thank Wei Zhang and Yansong Ren, who have been a source of encouragement and inspiration. Key R&D plan of Hainan Province, China (Item No. ZDYF2017112). we confirmed the study was carried out in compliance with the ARRIVE guidelines (http://www.nc3rs.org.uk/page.asp?id=1357).

Author contributions statement: H.H. conceived and designed the experiments, analyzed the data, wrote the paper, prepared figures and/or tables, reviewed drafts of the paper. J.Z.and H.T. conceived and designed the experiments, analyzed the data, prepared figures and/or tables, reviewed drafts of the paper. G.W. and W.W. analyzed the data, wrote the paper, reviewed drafts of the paper. H.H. and Y.F. performed the experiments, reviewed drafts of the paper. J.L. and M.D. conceived and designed the experiments, wrote the paper, reviewed drafts of the paper.

Conflicts of interest: The authors declare that there are no conflicts of interest regarding the publication of this paper.

References

1. Yuan, X., Arkonac, D. E., Chao, P. G. & Vunjak-Novakovic, G., Electrical stimulation enhances cell migration and integrative repair in the meniscus. **4**, 3674 (2014).
2. Jessica *et al.*, Time-dependent loss of mitochondrial function precedes progressive histologic cartilage degeneration in a rabbit meniscal destabilization model. (2017).
3. López-Franco, M. *et al.*, Meniscal degeneration in human knee osteoarthritis: in situ hybridization and immunohistochemistry study. *Archives of Orthopaedic & Trauma Surgery***136**, 175-183 (2016).
4. Aigner, T. *et al.*, Large-scale gene expression profiling reveals major pathogenetic pathways of cartilage degeneration in osteoarthritis. *Arthritis & Rheumatism: Official Journal of the American College of Rheumatology***54**, 3533-3544 (2006).
5. Brophy, R. H., Sandell, L. J., Cheverud, J. M. & Rai, M. F., Gene expression in human meniscal tears has limited association with early degenerative changes in knee articular cartilage. *Connect. Tissue Res.***58**, 295-304 (2017).
6. Sun, Y. & Mauerhan, D. R., Meniscal calcification, pathogenesis and implications. *Curr. Opin. Rheumatol.***24**, 152-157 (2012).
7. Sun, Y. *et al.*, Analysis of meniscal degeneration and meniscal gene expression. *BMC Musculoskel. Dis.***11**, 19 (2010).

8. Taylor, E. *et al.*, Sequence verification as quality-control step for production of cDNA microarrays. *Biotechniques***31**, 62-65 (2001).
9. Gupta, B., Sikander, M. & Jaggi, M., Overview of mucin (MUC13) in gastrointestinal cancers. *J Gastroenterol Dig Dis***1**, 18-19 (2016).
10. Sheng, Y. H. *et al.*, MUC1 and MUC13 differentially regulate epithelial inflammation in response to inflammatory and infectious stimuli. *Mucosal Immunol.***6**, 557-568 (2013).
11. Zhang, B. *et al.*, Investigation of the porcine MUC13 gene: isolation, expression, polymorphisms and strong association with susceptibility to enterotoxigenic Escherichia coli F4ab/ac. *Anim. Genet.***39**, 258-266 (2008).
12. Rokkanen, P., Paatsama, S. & Rissanen, P., The Influence of Certain Hormones on the Meniscus of the Femoro-tibial (Stifle) Joint: A histological and histo-quantitative study on young dogs. *J. Small Anim. Pract.***8**, 221-227 (1967).
13. Noone, T. J. *et al.*, Influence of canine recombinant somatotropin hormone on biomechanical and biochemical properties of the medial meniscus in stifles with altered stability. *Am. J. Vet. Res.***63**, 419-426 (2002).
14. Huang, H., Skelly, J. D., Ayers, D. C. & Song, J., Age-dependent changes in the articular cartilage and subchondral bone of C57BL/6 mice after surgical destabilization of medial meniscus. *Sci. Rep.-UK***7**, 42294 (2017).
15. Blanco, F. J., Ochs, R. L., Schwarz, H. & Lotz, M., Chondrocyte apoptosis induced by nitric oxide. *The American journal of pathology***146**, 75 (1995).
16. Shen, P., Nguyen, M., Fuchs, M., Reisener, M. J. & Löhning, M., TLR1/2 signaling impairs mitochondrial oxidative phosphorylation in human chondrocytes via the induction of nitric oxide. *Osteoarthr. Cartilage***28**, S119 (2020).
17. Kobayashi, K., Mishima, H., Hashimoto, S., Goomer, R. S. & Amiel, D., Chondrocyte apoptosis and regional differential expression of nitric oxide in the medial meniscus following partial meniscectomy. *J. Orthop. Res.***19**, 802-808 (2010).
18. Kao, X. B. *et al.*, SP600125 blocks the proteolysis of cytoskeletal proteins in apoptosis induced by gas signaling molecule (NO) via decreasing the activation of caspase-3 in rabbit chondrocytes. *Eur. J. Pharmacol.***824**, 40-47 (2018).
19. Kim, S., Hwang, S., Shin, D. Y., Kang, S. & Chun, J., p38 kinase regulates nitric oxide-induced apoptosis of articular chondrocytes by accumulating p53 via NFκB-dependent transcription and stabilization by serine 15 phosphorylation. *J. Biol. Chem.***277**, 33501-33508 (2002).
20. Relić, B. *et al.*, TNF-α protects human primary articular chondrocytes from nitric oxide-induced apoptosis via nuclear factor-κB. *Lab. Invest.***82**, 1661-1672 (2002).
21. Surendran, S. *et al.*, Anti-apoptotic Bcl-2 gene transfection of human articular chondrocytes protects against nitric oxide-induced apoptosis. *The Journal of Bone and Joint Surgery. British volume***88**, 1660-1665 (2006).
22. Shen, P., Nguyen, M., Fuchs, M., Reisener, M. J. & Löhning, M., TLR1/2 signaling impairs mitochondrial oxidative phosphorylation in human chondrocytes via the induction of nitric oxide. *Osteoarthr. Cartilage***28**, S119 (2020).
23. Yan *et al.*, Ligustilide attenuates nitric oxide-induced apoptosis in rat chondrocytes and cartilage degradation via inhibiting JNK and p38 MAPK pathways. *Journal of Cellular & Molecular Medicine* (2019).
24. Ramirez, G. A. *et al.*, Ion channels and transporters in inflammation: special focus on TRP channels and TRPC6. *Cells***7**, 70 (2018).
25. Oehler, B. *et al.*, Inflammatory pain control by blocking oxidized phospholipid-mediated TRP channel activation. *Sci. Rep.-UK***7**, 1-22 (2017).
26. Nalbantoglu, B., Tekir, S. D. & Ülgen, K. Ö., Wnt signaling network in homo sapiens. *Cell Metabolism–Cell Homeostasis Stress Response* (2012).
27. Wang, Q., Young, T. M., Mathews, M. B. & Pe Ery, T., Developmental regulators containing the I-mfa domain interact with T cyclins and Tat and modulate transcription. *J. Mol. Biol.***367**, 630-646 (2007).
28. van den Bosch, M. H. *et al.*, Induction of canonical Wnt signaling by synovial overexpression of selected Wnts leads to protease activity and early osteoarthritis-like cartilage damage. *The American journal of pathology***185**, 1970-1980

(2015).
29. Huang, H. *et al.*, Identification of pathways and genes associated with synovitis in osteoarthritis using bioinformatics analyses. *Sci. Rep.-UK***8**, 1-9 (2018).
30. Kitanaka, T. *et al.*, JNK activation is essential for activation of MEK/ERK signaling in IL-1β-induced COX-2 expression in synovial fibroblasts. *Sci. Rep.-UK***7**, 1-14 (2017).
31. Tornero-Esteban, P. *et al.*, Signature of microRNA expression during osteogenic differentiation of bone marrow MSCs reveals a putative role of miR-335-5p in osteoarthritis. *BMC Musculoskel. Dis.***16**, 182 (2015).

Figures

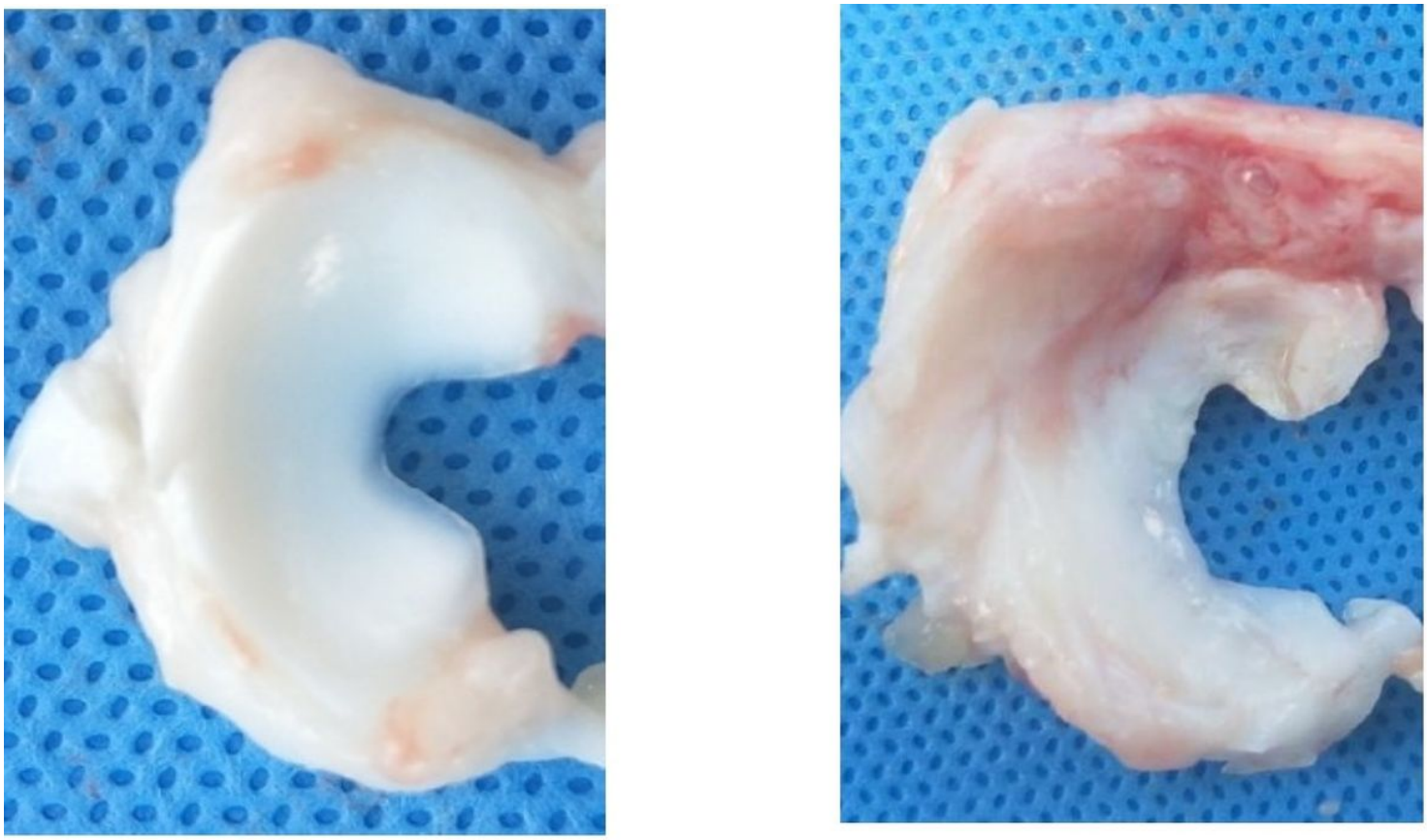

Figure 1

(a) In the normal meniscus group, the meniscus was crescent shaped, with complete and smooth surface, no tear, white color and good elasticity. And the medial part of the meniscus was thin and the lateral part was thick. (b) In the degenerative meniscus group, the color of the meniscus was light yellow, the elasticity was worse than that of the normal meniscus, the surrounding synovial membrane was congested and edema, the inner part was thinner with uneven wear, and the free edge was incomplete and cracked.

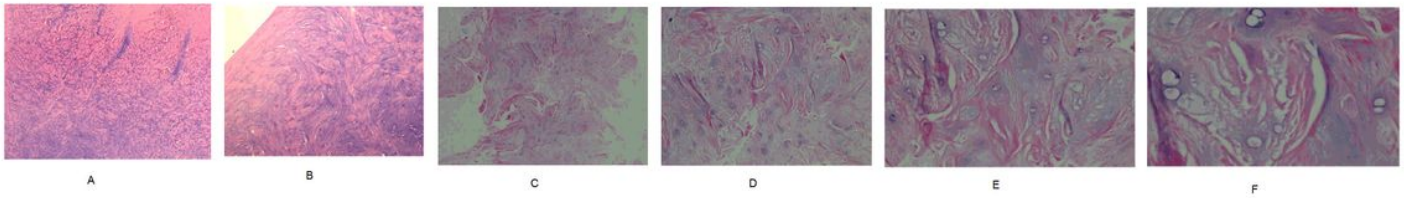

Figure 2

(a-b) The HE staining of normal meniscus tissue. The chondrocyte nucleus was large and round, the cell distribution was regular, the collagen fibers were abundant, and the fiber bundles were thick and neat. (c-f) The HE staining of degenerative meniscus. The arrangement of collagen fibers was disordered, the staining was uneven, and the arrangement was sparse; the chondrocytes were arranged disorderly and reduced, and the visible cells were swollen, the cartilage lacuna was reduced or disappeared, and the local area was fibrotic and hyalinized. a: x40, b: x100, c: x40, d: x100, e: x200, f: x400.

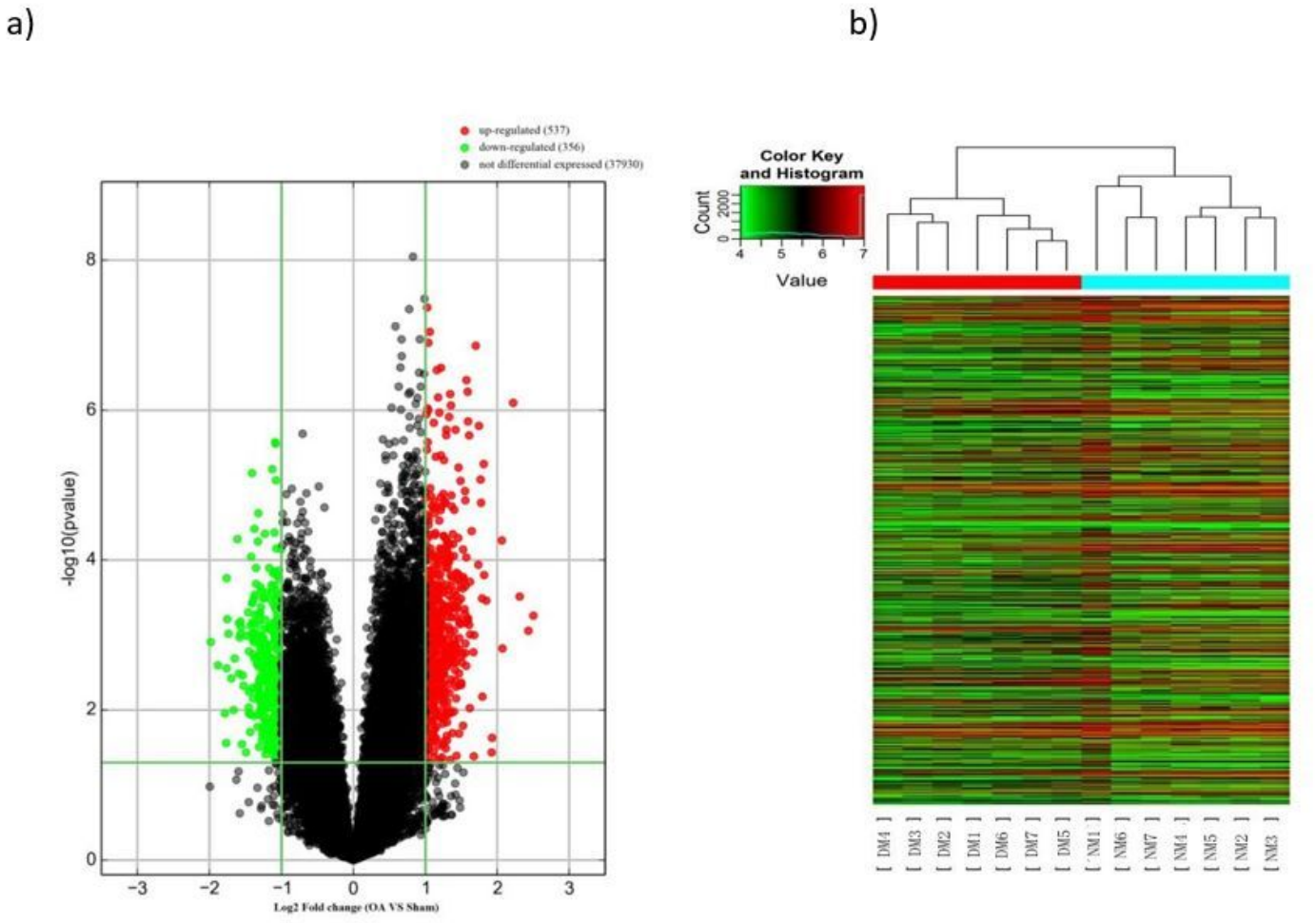

Figure 3

(a) The volcano plot. Red and green represent DEGs; the downregulated DEGs are green, and the upregulated DEGs are red. (b) The dendrogram. The ordinate represents the grouping information of the sample. Red indicates high relative expression and green indicates low relative expression. NM: normal meniscus; DM: degenerative meniscus.

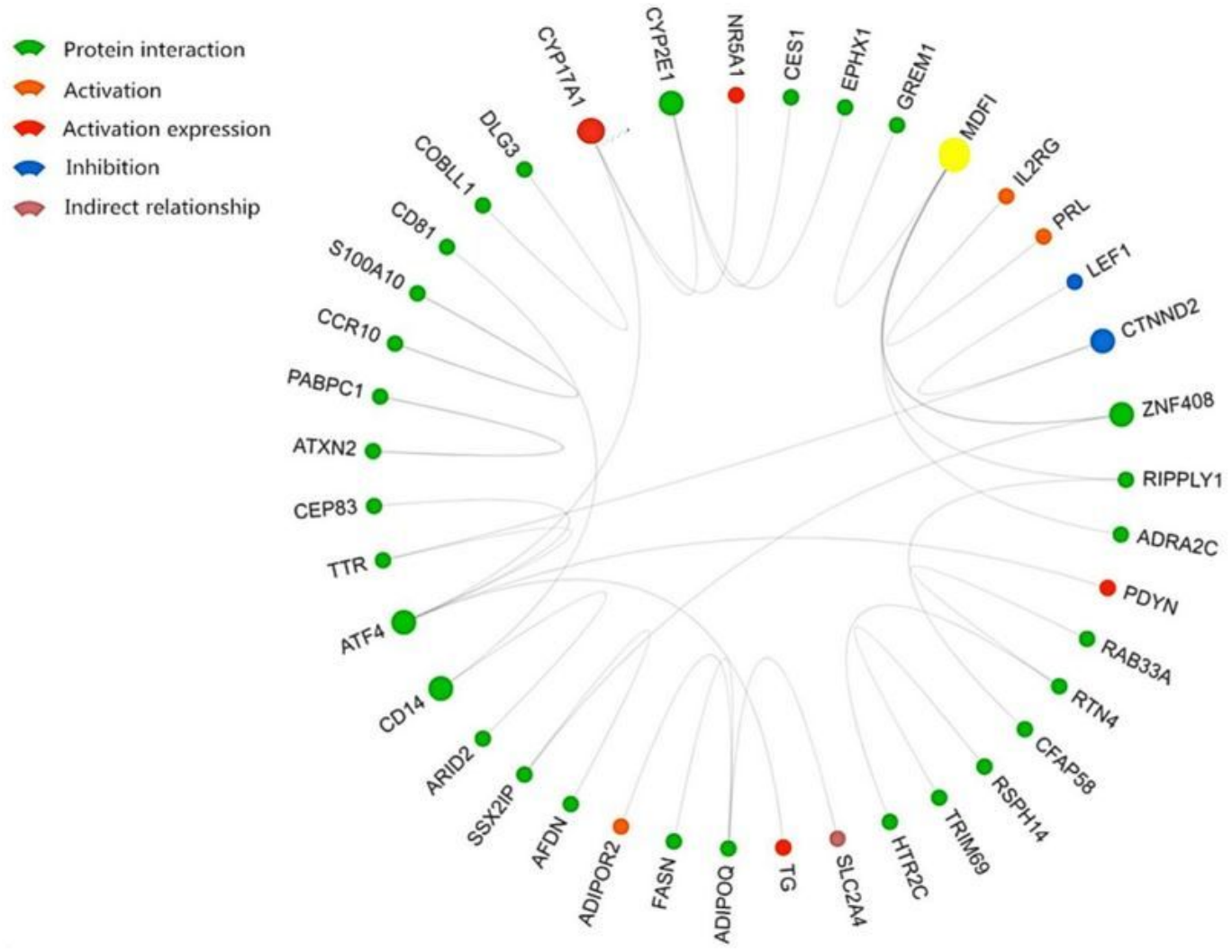

Figure 4

Interaction between core genes. Dots indicate core genes; lines between dots indicate relationships, and the colors of dots indicate specific relationships (see the icon in the upper left corner); larger dots indicate more relationships; yellow dots indicate genes with the most relationships (MDFI).

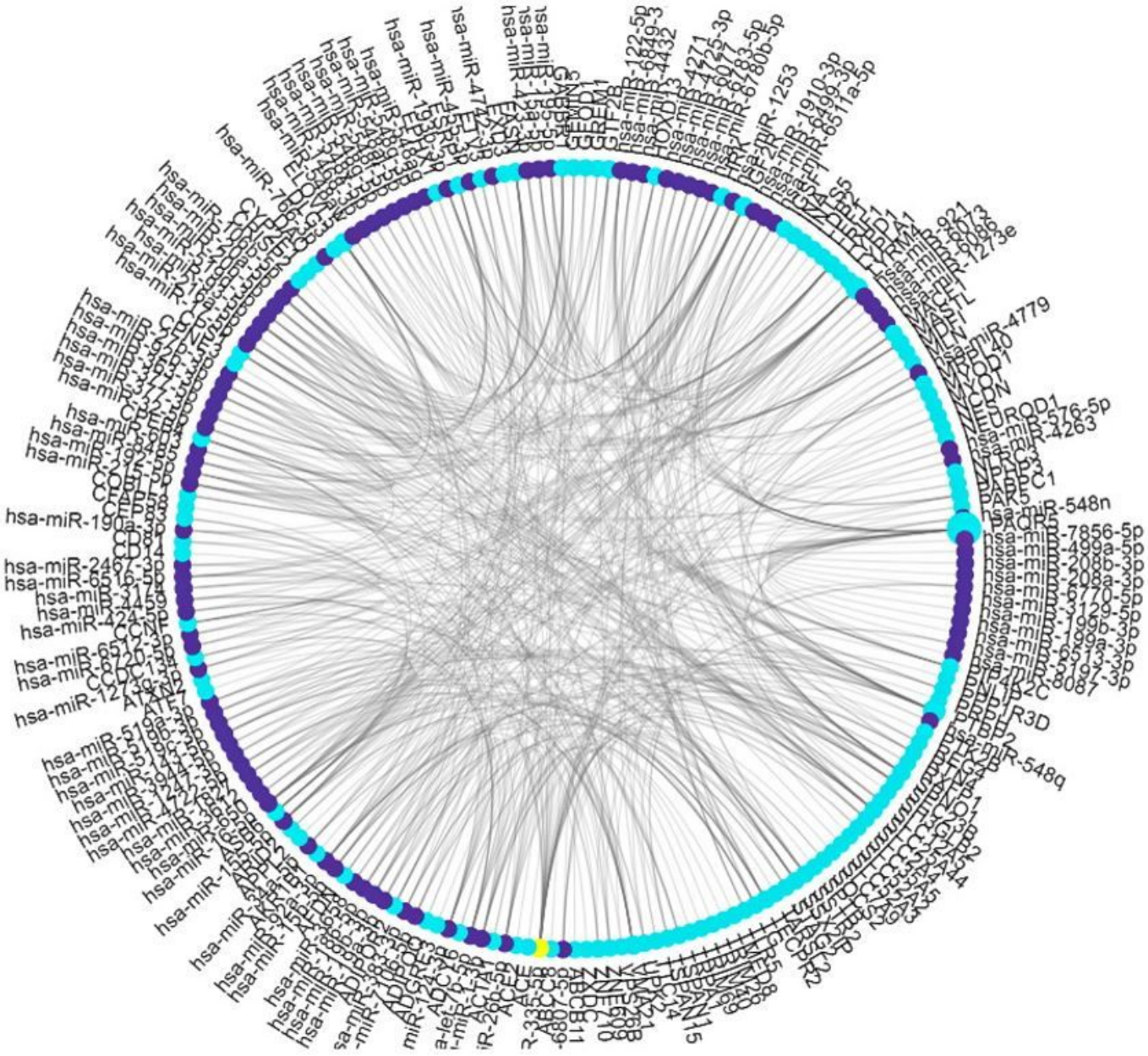

Figure 5

The relationship network between DEGs and miRNAs. Royal blue dots indicate DEGs; purple dots indicate miRNAs; larger dots indicate more relationships; yellow dots indicate miRNAs with the most relationships (miR-335-5p).

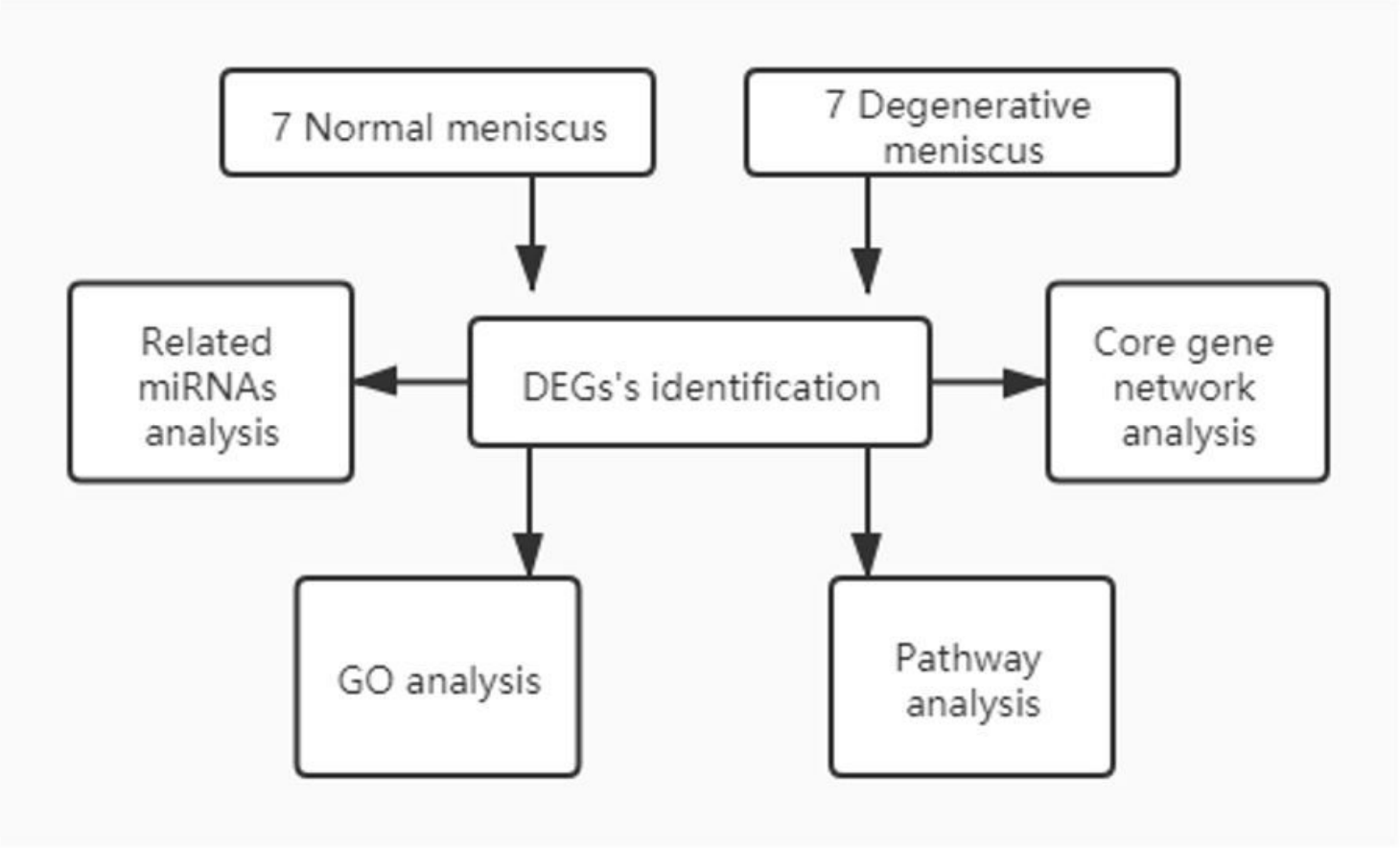

Figure 6

Flow diagram of the study design.